Solar Photovoltaic String Under Partial Condition With Irradiance

Anjali Verma[1], Mohd Javed Khan[2], Saif Ahmad[3]
[1, 2] Dept of ECE
[1, 2, 3] Integral University, Lucknow, U.P.

Abstract- *Partial shadowing has a significant impact on a solar system. It is implicitly assumed that the maximum power of a partially shaded photovoltaic system constantly declines as the shading heaviness increases since photovoltaic systems work by using sun irradiance to produce electricity. The literature has suggested that this might not be the case, nevertheless. When a specific critical point is reached, the maximum power of a partially shaded solar system under a set design and partial shading pattern can be significantly less susceptible to shading heaviness. In this essay, the effect of partial shading is examined, as well as the crucial location that lowers shading heaviness. In this study, solar modules are connected in series to create a photovoltaic string. The study of the P-V characteristic curve under various numbers of shaded modules and shading heaviness implies that when the irradiance of the shaded modules reaches a specific critical point, the photovoltaic string becomes insusceptible to shading heaviness. Depending on how many shaded modules there are, the critical point may change. With regard to various solar string diameters and the number of shadowed modules in the photovoltaic string, the equation developed in this study helps to identify the critical point.*

Keywords- Photovoltaic system, shading, irradiance, maximum power.

I. INTRODUCTION

Conventional electrical power generation based on coal-fired power plants introduces carbon emissions which cause air pollution to be released into the Earth's atmosphere. To tackle this problem, renewable energy is employed as an alternative mode of electrical power generation. Among the renewable energy options, photovoltaic solar power is getting more and more popular nowadays due to its abundantly available and inexhaustible nature [1–5]. The non-involvement of mechanical or moving parts in a photovoltaic power system also makes it more preferable than other renewable energy options [6]. In 2016, around 75 GW of solar photovoltaic capacity was installed worldwide, which is almost a 50% growth from about 50 GW in 2015 [7,8]. The significant growth in photovoltaic power systems promotes the popularity of photovoltaic power system research among renewable energy researchers.

Photovoltaic modules or solar panels are the most fundamental components in a photovoltaic power system which is used to convert solar energy to electrical power [9–13]. When a module is connected to a piece of measurement equipment, P-V characteristics will be obtained as illustrated in Figure 1 [14]. The P-V characteristics demonstrate the electrical power delivered by the photovoltaic module at different voltages.

In the presence of the P-V characteristics, the maximum power of the photovoltaic module can be tracked. For instance, the marked point in Figure 1.3shows the highest point of the P-V characteristics, which represents the maximum power delivered by the photovoltaic module[15]. The maximum power of the photovoltaic module is always harvested from the photovoltaic module for electricity generation purposes [16]. Therefore, it is important to determine the P-V characteristics of a photovoltaic module so that the maximum power can be tracked and harvested from the photovoltaic module.
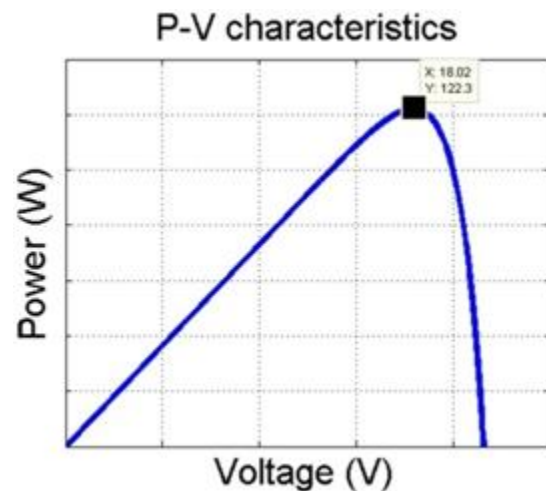
Figure 1. P-V characteristics of a photovoltaic module.

In a photovoltaic system, multiple photovoltaic modules are connected in series to form a photovoltaic string to achieve a required voltage and power output. To achieve an even higher power, these photovoltaic strings can be connected in parallel to form a photovoltaic array [17,18], as illustrated in Figure 2. In general, more than 1000 photovoltaic modules are employed in a megawatt-scale photovoltaic system to provide megawatts of electrical power production. These photovoltaic modules cannot only be connected in series as this will introduce an extremely high output voltage

which makes it unfit for grid-connected inverters and energy storage purposes. Therefore, parallel connection is employed, as well as series connection, to connect these photovoltaic modules. Usually, multiple photovoltaic strings are formed by connecting multiple photovoltaic modules in series. These photovoltaic strings are then connected in parallel to form the photovoltaic array in the megawatts scale photovoltaic plant. Similar to the photovoltaic module, the P-V characteristics of a photovoltaic string/array need to be determined in order to track and harvest the maximum power from the photovoltaic string/array.

(a)

(b)
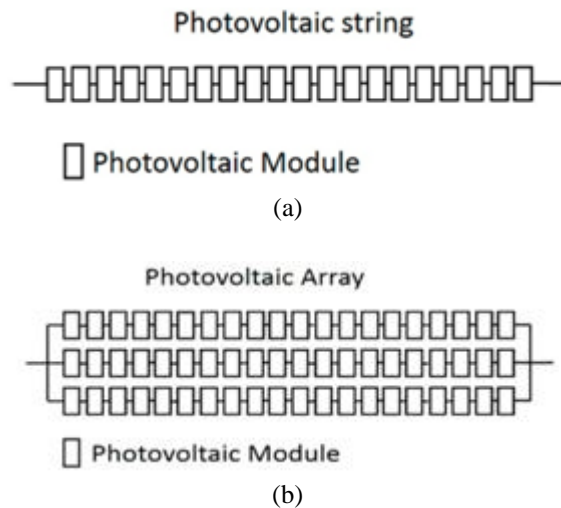
Figure 2. Photovoltaic system: (**a**) Photovoltaic string; (**b**) Photovoltaic array.

During a uniform irradiance condition, the P-V characteristics of a photovoltaic string exhibit one peak that resembles the P-V characteristics in Figure 1. The peak acts as the global peak which represents the maximum power of the photovoltaic string [19,20]. When partial shading takes place, multiple peaks appear on the P-V characteristics due to the use of a bypass diode [21–23]. Figure 3 shows the P-V characteristics of a photovoltaic string during a partial shading condition. The highest peak is the global peak which represents the maximum power of the photovoltaic string, while the others are the local peaks [24,25].

Apparently, a photovoltaic system is highly susceptible to partial shading [26–39]. During partial shading, the maximum power of a photovoltaic system can drop drastically, which significantly reduces the energy yield of the photovoltaic system. However, the susceptibility of partial shading to a photovoltaic system is not constant. The susceptibility of partial shading to a photovoltaic system can be varied due to the partial shading pattern and the connection employed to connect the photovoltaic modules in the photovoltaic system [26–29,32–38].
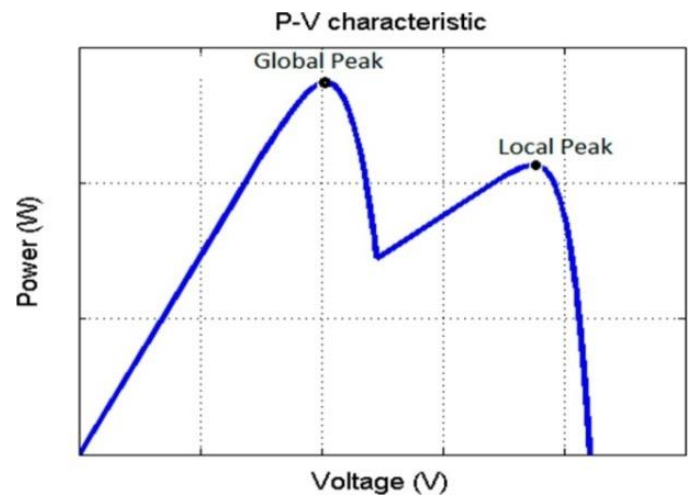
Figure 3. P-V characteristics of photovoltaic string under partial shading.

The experimental results in [26] suggested that under an identical partial shading pattern, the maximum power of a photovoltaic system should drop at a constant rate as the shading heaviness increases, as illustrated in Figure 1.6a. It means that under an identical partial shading pattern, a partially shaded photovoltaic system is always susceptible to the shading heaviness. This makes sense as the photovoltaic system relies on the solar irradiance to generate electrical power, and the maximum power of a partially shaded photovoltaic system should be lower and lower as the shading heaviness is getting heavier and heavier.

However, another phenomenon has been observed by S. Silvestre et al. [39]. S. Silvestre et al. discovered that a partially shaded photovoltaic system is not necessarily susceptible to the shading heaviness. They discovered that the maximum power of a partially shaded photovoltaic system decreases as the shading heaviness increases, as presented by the researchers in [26–38]. However, when the shading heaviness reaches a certain critical point, the maximum power remains unchanged even if the shading heaviness is getting heavier and heavier from that critical point, as illustrated in Figure 4 b. It means that the partially shaded photovoltaic system can become insusceptible to shading heaviness when the shading heaviness reaches a certain critical point. This finding is inspiring because a partially shaded photovoltaic system is commonly believed to always be susceptible to the shading heaviness.

(a)

(b)
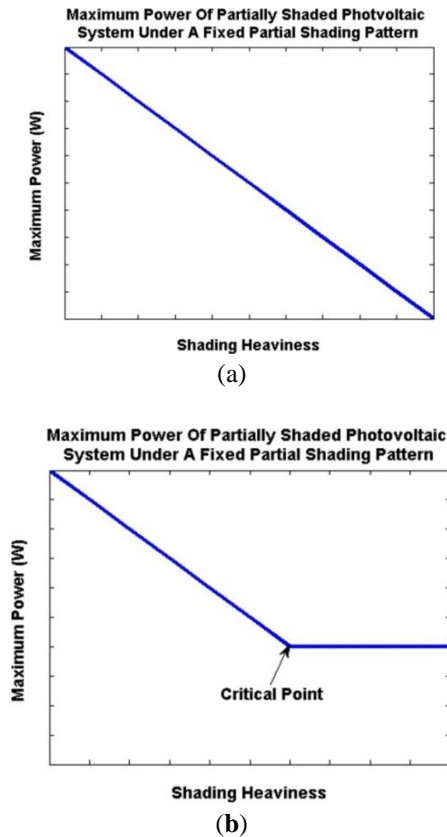
Figure 4. Maximum power of a partially shaded photovoltaic system under a fixed partial shading pattern

(**a**) as suggested by the experimental results in [26];
(b) as suggested by the experimental results in [39].

It is obvious that lots of research has been conducted on the impact of partial shading on the photovoltaic system throughout the years [26–38]. However, none of it has precisely presented the finding proposed in [39], which stated that the maximum power of a partially shaded photovoltaic system can become insusceptible to shading heaviness when the shading heaviness reaches a certain critical point. Therefore, it is a good area to further explore.

The finding proposed by [39] regarding the critical point is definitely inspiring. However, the experiment setup used in their research is a photovoltaic system that consists of nine photovoltaic modules only. They did not consider cases where a photovoltaic system consists of a greater number of photovoltaic modules. Besides that, the partial shading pattern and shading heaviness applied in their experiment are limited, which is insufficient to really conclude their finding. According to their result, the critical point can vary based on the number of shaded modules in the photovoltaic system. Therefore, an equation to determine the critical point for different numbers of shaded modules is highly expected. However, they did not formulate an equation

to determine the critical point. Furthermore, they did not verify whether the critical point is also applicable to different sized photovoltaic systems.

The aim of this research is to investigate the susceptibility of the shading heaviness to a partially shaded photovoltaic system and the critical point that decreases the susceptibility of shading heaviness using a photovoltaic system with a multiple number of photovoltaic modules and various partial shading conditions. Besides that, an equation to calculate the critical point is formulated in this research as well. Furthermore, the critical point equation is also verified with different sized photovoltaic systems.

With the increasingly environmental problems and shortages of traditional fossil fuels, solar energy as clean and renewable energy has attracted more and more attention. Photovoltaic power generation which has advantages of simplicity and convenience can directly convert solar energy to electrical energy. Coupled with the advancement of technology, such as improving conversion efficiency of solar cells and reducing the cost of devices, photovoltaic power generation is used more widely and has developed many different forms, including grid-connected or utility-interactive PV systems and stand-alone photovoltaic systems. But some undesirable problems such as hot spot and islanding effect occur correspondingly.

Hot spot occurs if the characteristics of solar cells mismatch are shaded or faulty, which reduces the short current of the shaded cell. Once the operating current of module or system exceeds the short current of the affected cell, the cell is forced into reverse bias and starts to consume the power generated by unshaded cells, resulting in overheating[42]. When the temperature of the shaded cell rises highly enough, the encapsulant, like EVA, will melt and the back sheet, like TPT, will be broken down, even leading to fire [43]. In general, bypass diodes are adopted to inhibit the shaded cell to crack and reduce the formation of hot spot. And the necessary parameters of bypass diodes and the number of cells in a string protected by a diode are determined by the parameters of normal cells [44].The typical group size is approximately 12–24 cells per bypass diode. However, these principles neglect whether or not the maximum heating power of the shaded cell can meet the requirement. It is also shown that bypass diodes are effective at preventing hot spot in short PV string lengths but cannot satisfy the demands in typical panel string lengths [45].

II. METHODOLOGY

A photovoltaic string consists of 4 photovoltaic modules and is used to conduct the experiment in this research. The photovoltaic modules have an open circuit voltage of 21.6 V, short circuit current of 7.34 A ideality factor of 1.5, and series resistance of 0 ohm. Temperature, T = 25∘C is used for all the case studies in the experiment. Each photovoltaic module in the photovoltaic string has one bypass diode.

There are three experiment setups developed using the photovoltaic string, including 1 modules shaded, 2 modules shaded and 3 modules shaded setups.

Table 1 shows all the conditions that applied to every experimental setup. In the experiment, the P-V characteristics of every experimental setup under all the applied conditions are determined.

Table1. Conditions applied to the experimental setups.

Conditions	Unshaded Modules Irradiance (W/m2)	Shaded Modules Irradiance (W/m2)
1	1200	1000
2	1200	800
3	1200	600
4	1200	400
5	1200	200
6	1200	100

A photovoltaic array that consists of parallel connected photovoltaic strings and is not used in this research. This is because a photovoltaic system with a higher degree of parallelism is less susceptible to partial shading [32]. Similar statements are also suggested in [33–40], which address the fact that a higher degree of parallelism in a photovoltaic system can reduce the susceptibility of partial shading. Therefore, a photovoltaic array that consists of parallelism is not used in this research. Photovoltaic string that is in a series connected configuration is used in this research.

The random partial shading patterns with multiple shading heaviness are not used in this research. These partial shading patterns occur due to an uneven cloud distribution. It is more likely to be experienced by a megawatts scale photovoltaic plant. The area of the coverage of the photovoltaic string is not as big as a megawatts scale photovoltaic system. Therefore, the random partial shading patterns with multiple shading heaviness are not considered in this research.

There is not a standard rule for choosing the photovoltaic system size to conduct the partial shading experiment. The size can be chosen based on the designer and researcher preferences. For instance, Hiren Patel and Vivek Agarwal [26] chose photovoltaic arrays that consist of 300, 900, and 1000 photovoltaic modules; R. Ahmad et al. [29] chose photovoltaic arrays that consist of 20 and 25 photovoltaic modules; S. Silvestre et al. [39] chose a photovoltaic array consisting of nine photovoltaic modules, and so on. Regardless of the chosen size of the photovoltaic system, the experimental outcome should be applicable in certain ways to a megawatts scale photovoltaic plant as tacitly assumed among the researchers [26–39].

A photovoltaic string model is developed to carry out the experiment. A solar cell block from the Sim Electronics block set is used to develop the photovoltaic string model. This method of modelling has been used by J. C. Teo et al. to develop a photovoltaic string model [11]. They have conducted practical measurements to validate the photovoltaic string model in their research. Hence, it makes sense to use this method to develop the photovoltaic string model for the experiment.

The solar cell block is set to a five-parameter configuration m which is defined in Equations (1) and (2), where I is the output current, I_{PH} is the photo-generated current, I_O is the diode saturation current, V is the output voltage, R_S is the series resistance, N_S is the number of cells, V_T is the junction thermal voltage, A is the ideality factor, k is the Boltzman constant ($1.3806503 \times 10^{-23}$ J/K), T is the cell temperature, and q is the electron charge ($1.6021765 \times 10^{-19}$ C).

$$I = I_{PH} - I_0 exp\left(\frac{V+IR_S}{N_S V_T} - 1\right) \tag{1}$$

$$V_T = \frac{AKT}{q} \tag{2}$$

The short circuit current, open circuit voltage, series resistance, and ideality factor of the solar cell block are set according to the experiment requirements. To implement the bypass diode, the diode block from the Simscape block set is connected in antiparallel with the solar cell block, as shown in Figure 6.
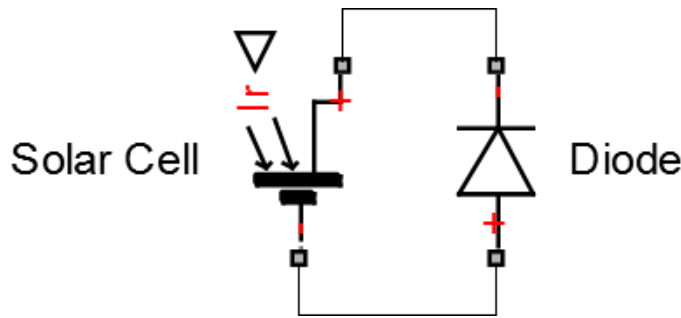
Figure 5. Solar cell block with bypass diode.

The architecture in Figure 5 represents a photovoltaic cell with a bypass diode. The architecture is duplicated to one sets, and these one sets of architecture are then connected in series to form a photovoltaic string model which consists of 4 photovoltaic modules that are required for the experiment. The photovoltaic string model is made into a single block known as PV string, as shown in Figure 6.
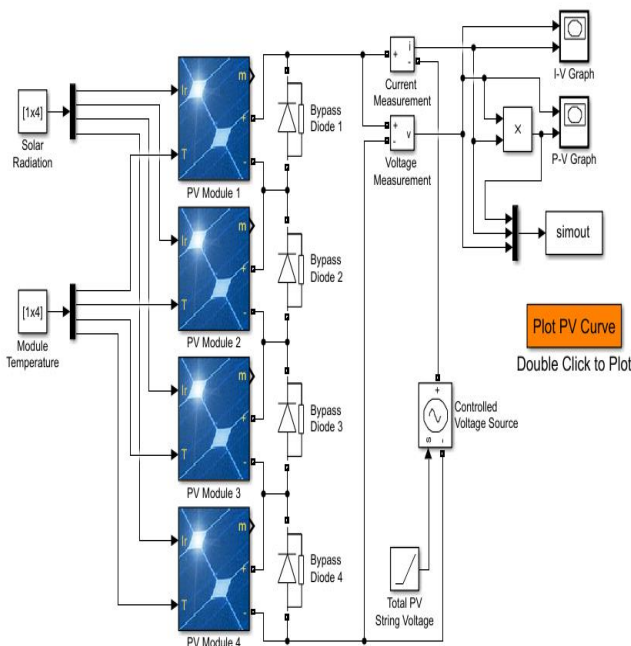

Figure 6. Photovoltaic string model.

Figure 6 shows the entire photovoltaic string model that was developed to carry out the experiment. The PV string block is the model for the photovoltaic string. It has 4 inputs which control the irradiance of every particular photovoltaic module in the photovoltaic string. The Control Unit block sets the unshaded modules irradiance, shaded modules irradiance, and number of the shaded modules in the PV string based on the parameter in the Unshaded Irr, Shaded Irr, and Shade Module block, respectively.

During the simulations, the Controlled Current Source block sweeps the output current of the photovoltaic

string. The Voltage Sensor block measures the output voltage of the photovoltaic string. The Product block multiplies the output voltage and output current of the photovoltaic string to obtain the output power of the photovoltaic string. The To Workspace block sends the output power and output voltage of the photovoltaic string to the MATLAB (R2014a, MathWorks, Natick, MA, USA) workspace to plot the P-V characteristics curve.

Basically, the developed photovoltaic string model shown in Figure 6 is developed by cascading and extending the photovoltaic string model proposed by J. C. Teo et al. [11]. It is common practice to develop a larger scale photovoltaic system model by cascading and extending the validated small-scale photovoltaic system model [26]. The larger scale model that is developed by cascading and extending the validated small-scale model should give appropriate results for analysis purposes, as suggested by [26,39]. The method in [26] has also been applied by another researcher [29] to conduct a partial shading experiment.

The experiment can be conducted using the photovoltaic string model shown in Figure 3.2. To conduct the experiment for the three modules shaded setup, the Unshade Irr block is set to 1200 while the Shaded Module block is set to one. These settings configure the photovoltaic string to a three modules shaded setup with the unshaded modules irradiance fixed at 1200 W/m2. The Shade Irr block is set to 1000 to apply the condition 1 in Table 2 to the one modules shaded setup. Simulation performed under these setting generates the P-V characteristics of the one modules shaded setup under condition 1. To obtain the P-V characteristics of the one modules shaded setup under all the conditions in Table2, 6 simulations are performed with the Shade Irr block set to 100, 200, 400, , 600, 800 and 1000, respectively.

Similar procedures are applied to conduct the experiment for the two modules shaded, and three modules shaded setup. For instance, for the two modules shaded setup, the Unshade Irr block is set to 1200 while the Shade Module block is set to 1000 W/m2. These settings configure the photovoltaic string to the two modules shaded setup with the unshaded module irradiance fixed at 1000 W/m2. To obtain the P-V characteristics of the two modules shaded setup under all the conditions in Table3, 16simulations are performed with the Shade Irr block set to 100, 200, 400, , 600, 800 and 1000, respectively.

To conduct the experiment for the three modules shaded setup, the Unshade Irr block is set to 1200 while the Shade Modules block is set to 1000W/m2. The simulations are performed with the Shade Irr block set to 100, 200, 400, 600,

800 and 1000, respectively, to obtain the P-V characteristics of the three modules shaded setup under the Tables 3.2–3.4show the parameters set in the model in Figure 6 to conduct the experiment for the one modules shaded, two modules shaded and three modules shaded setups.

Table 2. Parameters set in the model shown in Figure 6 to conduct the experiment for the one modules shaded setup with Parameter Set in Shade Module Block=1

Condition Applied to the Experiment Setup	Parameter Set in Unshade Irr Block	Parameter Set in Shade Irr Block
Condition 1	1200	1000
Condition 2	1200	800
Condition 3	1200	600
Condition 4	1200	400
Condition 5	1200	200
Condition 6	1200	100

Table 3. Parameters set in the model shown in Figure 6 to conduct the experiment for the two modules shaded setup Parameter Set in Shade Module Block=2

Condition Applied to the Experiment Setup	Parameter Set in Unshade Irr Block	Parameter Set in Shade Irr Block
Condition 1	1200	1000
Condition 2	1200	800
Condition 3	1200	600
Condition 4	1200	400
Condition 5	1200	200
Condition 6	1200	100

Table 4. Parameters set in the model shown in Figure 6 to conduct the experiment for the three modules shaded setup with Parameter Set in Shade Module Block=3

Condition Applied to the Experiment Setup	Parameter Set in Unshade Irr Block	Parameter Set in Shade Irr Block
Condition 1	1200	1000
Condition 2	1200	800
Condition 3	1200	600
Condition 4	1200	400
Condition 5	1200	200
Condition 6	1200	100

The experiment considers lots of partial shading conditions, including lightly shaded, heavily shaded, a small number of modules shaded, a big number of modules shaded, and lots of shading heaviness conditions. These partial shading conditions pretty much cover all the possible partial shading conditions that might be experienced by a photovoltaic string at the site. Hence, the data collected in the experiment should be sufficient to conclude the critical points of a photovoltaic string, as well as to formulate the equation to determine the critical points of a photovoltaic string. However, more simulation work is required to conduct the experiment as it involves a huge number of partial shading conditions.
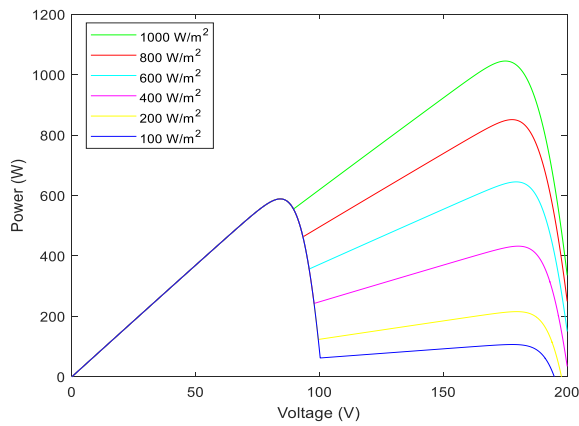
III. RESULT

Figure 7 shows the P-V characteristics of the one modules shaded setup. Figure 4.1a represents the P-V characteristics when the shaded modules irradiance is between 500 and 900 W/m2. Figure 4.1b illustrates the P-V characteristics when the shaded modules irradiance is between 0 and 400 W/m2. Considering the one modules shaded setup in Figure 7a, the higher voltage peak of the P-V characteristics is higher than the lower voltage peak when the shaded module irradiance is between 800 and 900 W/m2.
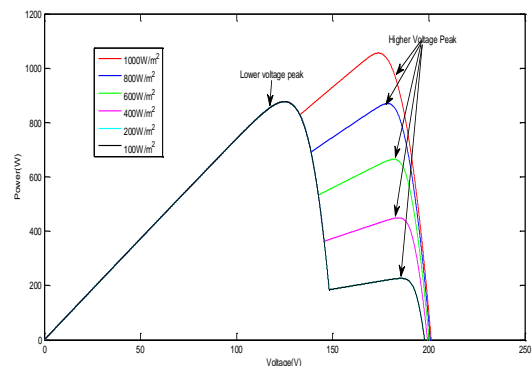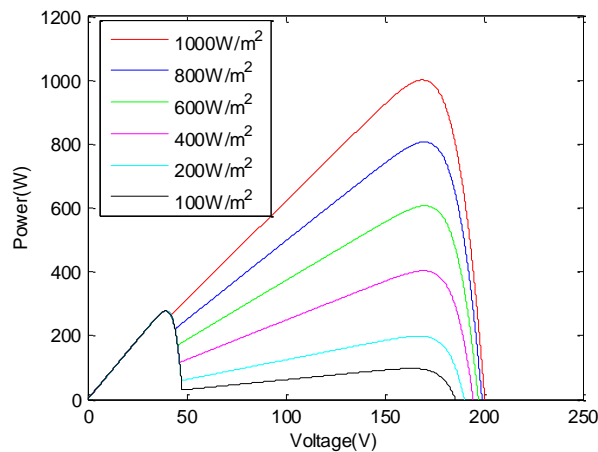

Figure 7. P-V characteristics of the one modules shaded setups: shaded modules irradiance is between 1000 and 100 W/m2;

Figure 8 shows the P-V characteristics of the two modules shaded setup. Figure 8a represents the P-V characteristics when the shaded modules irradiance is between 500 and 900 W/m2. Figure 8b illustrates the P-V characteristics when the shaded modules irradiance is between 0 and 400 W/m2. Similar situations are observed in the two modules shaded setup shown in Figure 8, where the higher voltage peak acts as the global peak when the shaded modules irradiance is above a certain level. The higher voltage peak reduces as the shaded modules irradiance decreases.

Figure 8. P-V characteristics of the two modules shaded setups: shaded modules irradiance is between 1000 and 100 W/m2;

Figure 9 shows the P-V characteristics of the three modules shaded setup. The similar situation that is observed in the one and two modules shaded setups is also observed in the three module shaded setups shown in Figures 9 . The higher voltage peak acts as the global peak when the shaded modules irradiance is above a certain level.

Figure 9. P-V characteristics of the three modules shaded setups: shaded modules irradiance is between 1000 and 100 W/m2

Tables 5– 8 are tabulated based on the data on the P-V characteristics of Figures 7–9 which show the maximum power and maximum power delivery voltage of all the experimental setups under the applied conditions.

Table 5. Maximum powers of the one modules shaded setup with Unshaded Module Irradiance (1000 W/m^2)

Unshaded Module Irradiance (W/m2)	shaded Module Irradiance (W/m2)	Maximum Power (W)	Delivery Voltage (V)
1200	1000	1055.8	174
1200	800	876.85	125
1200	600	876.84	125
1200	400	876.83	125
1200	200	876.82	125
1200	100	876.81	125

Table 6. Maximum powers of the two modules shaded setup with Unshaded Module Irradiance (1000 W/m^2)

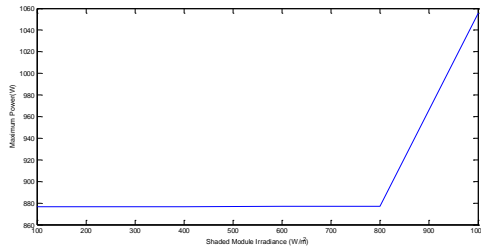| Unshaded Module Irradiance (W/m2)	shaded Module Irradiance (W/m2)	Maximum Power (W)	Delivery Voltage (V)
1200	1000	1025.6	171
1200	800	835.695	173
1200	600	633.548	176
1200	400	577.055	82.13
1200	200	577.038	82.13
1200	100	577.029	82.13

**Table 7.** Maximum powers of the Three modules shaded setup with Unshaded Module Irradiance (1000 W/m^2)

Unshaded Module Irradiance (W/m2)	shaded Module Irradiance (W/m2)	Maximum Power (W)	Delivery Voltage (V)
1200	1000	1001.1	170.1
1200	800	806.898	170.2
1200	600	606.607	171.9
1200	400	403.088	171.8
1200	200	277.268	39.43
1200	100	277.255	39.43

By using the maximum powers and shaded modules irradiance in Table 5, a graph such as that illustrated in Figure 10 can be plotted. It shows the relationship between the maximum powers and the shaded modules irradiance of the one modules shaded setup.

Figure 10. Maximum power versus shaded modules irradiance (one modules shaded).

Similar procedures are applied to Tables 6–7 to obtain the relationship between the maximum powers and the shaded modules irradiance for the 2 and 3 modules shaded setups. Figure 11 shows the relationship between the shaded modules irradiance and the maximum powers for all the experimental setups.
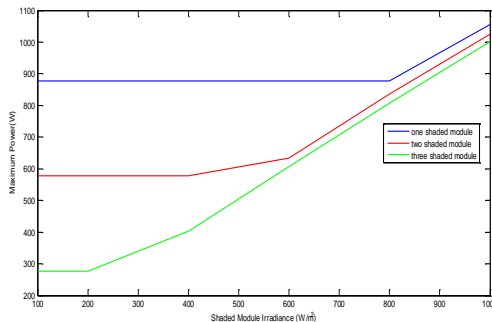
Figure 11. Maximum power versus shaded modules irradiance (all experiment setups).

V. CONCLUSION

Photovoltaic systems are highly susceptible to partial shading. The maximum power of a photovoltaic system can reduce drastically when partial shading takes place. The susceptibility of partial shading can vary based on the partial shading patterns, shading heaviness, and the configuration employed in connecting all the photovoltaic modules in the photovoltaic system. Under a fixed configuration and partial shading pattern, the maximum power of a partially shaded photovoltaic system is tacitly assumed to decrease at a constant rate as the shading heaviness increases. This tacit assumption is proposed based on the functionality of a photovoltaic system that relies on solar irradiance to generate electrical power. However, some researchers discovered that the maximum power under a fixed configuration and partial shading pattern can be highly insusceptible to shading heaviness when a certain critical point is met. Furthermore, the critical point can vary based on the number of shaded modules in a photovoltaic system. The novelty of this research includes the formulation of the equation to determine the critical point that is applicable to different photovoltaic system sizes and numbers of shaded modules in a photovoltaic system. Besides that, the equation has been verified with different sized photovoltaic systems as well. When 40% of photovoltaic modules in the photovoltaic system are shaded under an identical partial shading pattern, the maximum power drops by approximately 16.27% for every 100 W/m2 drop in the shaded module irradiance as the shaded modules irradiance lies between 1000 and 600 W/m2. However, when the shaded modules irradiance lies between 600 and 100 W/m2, the maximum power drops only by 9.07% for every 100 W/m2 drop in the shaded module irradiance..

REFERENCES

[1] K. J. R. Liu, A. K. Sadek, W. Su, and A. Kwasinski, Cooperative Communications and Networking. New York City, NY, USA: Cambridge University Press, 2009.

[2] P. N. Son and H. Y. Kong, "Cooperative communication with energy-harvesting relays under physical layer security," IET Commun., vol. 9, no. 17, pp. 2131–2139, Nov. 2015.

[3] R. Fan, J. Cui, S. Jin, K. Yang, and J. An, "Optimal node placement and resource allocation for UAV relaying network," IEEE Commun. Lett., vol. 22, no. 4, pp. 808–811, Apr. 2018.

[4] M. Ju and H.-C. Yang, "Optimum design of energy harvesting relay for two-way decode-and forward relay networks under max-min and max-sum criterions," IEEE Trans. Commun., vol. 67, no. 10, pp. 6682–6697, Oct. 2019.

[5] K. Sultan, "Best relay selection schemes for NOMA based cognitive relay networks in underlay spectrum sharing," IEEE Access, vol. 8, pp. 190 160–190 172, 2020.

[6] A. Sendonaris, E. Erkip, and B. Aazhang, "User cooperation diversity-part I: System description,"IEEE Trans. Commun., vol. 51, no. 11, pp. 1927–1938, Nov. 2003.

[7] "User cooperation diversity-part II: Implementation aspects and performance analysis," IEEE Trans. Commun., vol. 51, no. 11, pp. 1939–1948, Nov. 2003.

[8] R. U. Nabar, H. Bolcskei, and F. W. Kneubuhler, "Fading relay channels: Performance limits and space-time signal design," IEEE J. Sel. Areas Commun., vol. 22, no. 6, pp. 1099–1109, Aug. 2004.

[9] H. Cui, L. Song, and B. Jiao, "Multi-pair two-way amplify-and-forward relaying with very large number of relay antennas," IEEE Trans. Wireless Commun., vol. 13, no. 5, pp. 2636–2645, May 2014.

[10] S. Luo and K. C. Teh, "Amplify-and-forward based two-way relay arq system with relay combination,"IEEE Commun. Lett., vol. 19, no. 2, pp. 299–302, Feb. 2015.

[11] D. Li, "Amplify-and-forward relay sharing for both primary and cognitive users," IEEE Trans. Veh.Technol., vol. 65, no. 4, pp. 2796–2801, Apr. 2016.

[12] Y. Dong, M. J. Hossain, and J. Cheng, "Performance of wireless powered amplify and forward relaying over Nakagami-mfading channels with nonlinear energy harvester," IEEE Commun. Lett.,vol. 20, no. 4, pp. 672–675, Apr. 2016.

[13] S. Li, K. Yang, M. Zhou, J. Wu, L. Song, Y. Li, and H. Li, "Full-duplex amplify-and-forward relaying: Power and location optimization," IEEE Trans. Veh. Technol., vol. 66, no. 9, pp. 8458– 8468, Sep. 2017.

[14] K. M. Rabie and B. Adebisi, "Enhanced amplify-and-forward relaying in non-Gaussian PLC networks,"IEEE Access, vol. 5, pp. 4087–4094, 2017.

[15] L. Jiang and H. Jafarkhani, "mmWave amplify-and-forward MIMO relay networks with hybrid precoding/combining design," IEEE Trans. Wireless Commun., vol. 19, no. 2, pp. 1333–1346, Feb. 2020.

[16] A. S. Ibrahim, A. K. Sadek, W. Su, and K. J. R. Liu, "Cooperative communications with relay selection:When to cooperate and whom to cooperate with?" IEEE Trans. Wireless Commun., vol. 7, no. 7, pp. 2814–2827, Jul. 2008.

[17] M. R. Bhatnagar, R. K. Mallik, and O. Tirkkonen, "Performance evalution of best-path selection in a multihop decode-and-forward cooperative system," IEEE Trans. Veh. Technol., vol. 65, no. 4, pp.2722–2728, Apr. 2016.

[18] Y. Gu and S. Aissa, "RF-based energy harvesting in decode-and-forward relaying systems: Ergodic and outage capacities," IEEE Trans. Wireless Commun., vol. 14, no. 11, pp. 6425–6434, Nov. 2015.

[19] G. T. Djordjevic, K. Kansanen, and A. M. Cvetkovic, "Outage performance of decode-and-forward cooperative networks over Nakagami-m fading with node blockage," IEEE Trans. Wireless Commun.,vol. 15, no. 9, pp. 5848–5860, Sep. 2016.

[20] H. Liu, Z. Ding, K. J. Kim, K. S. Kwak, and H. V. Poor, "Decode-and-forward relaying for cooperative NOMA systems with direct links," IEEE Trans. Wireless Commun., vol. 17, no. 12, pp.8077–8093, Dec. 2018.

[21] R. Fan, S. Atapattu, W. Chen, Y. Zhang, and J. Evans, "Throughput maximization for multihop decode-and-forward relay network with wireless energy harvesting," IEEE Access, vol. 6, pp.24 582–24 595, 2018.

[22] O. M. Kandelusy and S. M. H. Andargoli, "Outage performance of decode-and-forward (DF)-based multiuser spectrum sharing relay system with direct link in the presence of primary users' power,"IET Commun., vol. 12, no. 3, pp. 246–254, Feb. 2018.

[23] E. Li, X. Wang, Z. Wu, S. Hao, and Y. Dong, "Outage analysis of decode-and-forward two-way relay selection with different coding and decoding schemes," IEEE Syst. J., vol. 13, no. 1, pp.125–136, Mar. 2019.

[24] M. Asadpour, B. Van den Bergh, D. Giustiniano, K. A. Hummel, S. Pollin, and B. Plattner, "Micro aerial vehicle networks: an experimental analysis of challenges and opportunities," IEEE Commun.Mag., vol. 52, no. 7, pp. 141–149, Jul. 2014.

[25] K. Namuduri, S. Chaumette, J. H. Kim, and J. P. G. Sterbenz, UAV Networks and Communications. Cambridge University Press, 2017.

[26] K. P. Valavanis and G. J. Vachtsevanos, Handbook of Unmanned Aerial Vehicles. Springer, 2015.

[27] F. Ono, H. Ochiai, and R. Miura, "A wireless relay network based on unmanned aircraft system with rate optimization," IEEE Trans. Wireless Commun., vol. 15, no. 11, pp. 7699–7708, Nov. 2016.

[28] M. M. Azari, F. Rosas, K.-C. Chen, and S. Pollin, "Ultra reliable UAV communication using altitude and cooperation diversity," IEEE Trans. Commun., vol. 66, no. 1, pp. 330–344, Jan. 2018.

[29] M. M. Azari, F. Rosas, and P. Sofie, "Cellular connectivity for UAVs: Network modeling, performance analysis, and design guidelines," IEEE Trans. Wireless Commun., vol. 18, no. 7, pp.3366–3381, Jul. 2019.

[30] W. Wang, X. Li, M. Zhang, K. Cumannan, D. W. K. Ng, G. Zhang, J. Tang, and O. A. Dober, "Energy-constrained UAV-assisted secure communications with position optimization and cooperative jamming," IEEE Trans. Commun., vol. 68, no. 7, pp. 4476–4489, Jul. 2020.

[31] H. Shakhatreh, A. H. Sawalmeh, A. Al-Fuqaha, Z. Dou, E. Almaita, I. Khalil, N. S. Othman,A. Khreishah, and M. Guizani, "Unmanned aerial vehicles (UAVs): A survey on civil applications and key research challenges," IEEE Access, vol. 7, pp. 48 572–48 634, 2019.

[32] W. Ejaz, M. A. Azam, S. Saadat, F. Iqbal, and A. Hanan, "Unmanned aerial vehicle enabled IoT platform for disaster management," Energies, vol. 12, no. 14, p. 2706, Jul. 2019.

[33] Y. Zeng, R. Zhang, and T. J. Lim, "Wireless communications with unmanned aerial vehicles: opportunities and challenges," IEEE Commun. Mag., vol. 54, no. 5, pp. 36–42, May 2016.

[34] J. Zhao, F. Gao, Q. Wu, S. Jin, Y. Wu, and W. Jia, "Beam tracking for UAV mounted Sat Com on the-move with massive antenna array," IEEE J. Sel. Areas Commun., vol. 36, no. 2, pp. 363–375,Feb. 2018.

[35] Y. Zeng, R. Zhang, and T. J. Lim, "Throughput maximization for UAV-enabled mobile relaying

systems," IEEE Trans. Commun., vol. 64, no. 12, pp. 4983–4996, Dec. 2016.

[36] Y. Zhang, Z. Mou, F. Gao, L. Xing, J. Jiang, and Z. Han, "Hierarchical deep reinforcement learning for backscattering data collection with multiple UAVs," IEEE Internet Things J., vol. 8, no. 5, pp.3786–3800, Mar. 2021.

[37] J. Zhao, Y. Wang, Z. Fei, X. Wang, and Z. Miao, "NOMA-aided UAV data collection system: Trajectory optimization and communication design," IEEE Access, vol. 8, pp. 155 843–155 858,2020.

[38] F. Luo, C. Jiang, J. Du, J. Yuan, Y. Ren, S. Yu, and M. Guizani, "A distributed gateway selection algorithm for UAV networks," IEEE Trans. Emerg. Topics Comput., vol. 3, no. 1, Mar. 2015.

[39] R. Duan, J. Wang, C. Jiang, Y. Ren, and L. Hanzo, "The transmit-energy vs computation-delay trade-off in gateway-selection for heterogenous cloud aided multi-UAV systems," IEEE Trans.Commun., vol. 67, no. 4, pp. 3026–3039, Apr. 2019.

[40] M. Vaezi, R. Schober, Z. Ding, and H. V. Poor, "Non-orthogonal multiple access: Common myths and critical questions," IEEE Wireless Commun., vol. 26, no. 5, pp. 174–180, Oct. 2019.

[41] M. Vaezi and H. V. Poor, "NOMA: An information-theoretic perspective," in Multiple Access Techniques for 5G Wireless Networks and Beyond, M. Vaezi, Z. Ding, and H. V. Poor, Eds. Cham:Springer International Publishing, 2019, pp. 167–193.

[42] F. Mokhtari, M. R. Milli, F. Eslami, F. Ashtiani, B. Makki, M. Mirmohseni, M. Nasiri-Kenari, and T. Svensson, "Download elastic traffic rate optimization via NOMA protocols," IEEE Trans. Veh. Technol., vol. 68, no. 1, pp. 713–727, Jan. 2019.

[43] Z. Ding, M. Peng, and H. V. Poor, "Cooperative non-orthogonal multiple access in 5G systems,"IEEE Commun. Lett., vol. 19, no. 8, pp. 1462–1465, Aug. 2015.

[44] S. M. R. Islam, N. Avazov, O. A. Dobre, and K.-s. Kwak, "Power-domain non-orthogonal multiple access (NOMA) in 5G systems: Potentials and challenges," IEEE Commun. Surveys Tuts., vol. 19, no. 2, pp. 721–742, Second quarter 2017.

[45] 3GPP, "Study on network-assisted interference cancellation and suppression (NAICS) for LTE v.12.0.1," 3rd Generation Partnership Project (3GPP), Sophia Antipolis, France, Rep. TR 36.866, Mar. 2014.

[46] Media Tek, "Study on downlink multiuser superposition transmission (MUST) for LTE," 3rd Generation Partnership Project (3GPP), Hsinchu, Taiwan, Rep. TR 36.859, Apr. 2015.

[47] B. Wu, J. Chen, J. Wu, and M. Cardei, "A survey of attacks and countermeasures in mobile ad hoc networks,"

in Wireless Network Security, Y. Xiao, X. S. Shen, and D.-Z. Du, Eds. Boston, MA,USA: Springer, 2007, ch. 5, pp. 103–135.

[48] Y. Wang, G. Attebury, and B. Ramamurthy, "A survey of security issues in wireless sensor networks,"IEEE Commun. Surveys Tuts., vol. 8, no. 2, pp. 2–23, Second Quarter 2006.

[49] T. T. Karygiannis and L. Owens, "Wireless network security: 802.11, bluetooth and handheld devices," Gaithersburg, MD, USA, Nov. 2002.

[50] P. W. Shor, "Algorithms for quantum computation: discrete logarithms and factoring," in Proc.IEEE Annu. Symp. Found. of Comput. Sci. (FOCS), Santa Fe, NM, USA, Nov. 1994.

[51] R. K. Nichols and P. C. Lekkas, Wireless Security: Models, Threats, and Solutions. New York,NY, USA: McGraw-Hill, 2002.

[52] M. Bloch and J. Barros, Physical-Layer Security: From Information Theory to Security Engineering.Cambridge, United Kingdom: Cambridge University Press, 2011.

[53] A. D. Wyner, "The wire-tap channel," Bell Syst. Tech. J., vol. 54, no. 8, pp. 1355–1387, 1975.